Ultrastructure of Unit Fragments of the Skeleton of the Human Erythrocyte Membrane

BETTY W. SHEN, ROBERT JOSEPHS, and THEODORE L. STECK
Department of Biophysics and Theoretical Biology and Department of Biochemistry, University of Chicago, Chicago, Illinois 60637

ABSTRACT We have examined fragments of the filamentous network underlying the human erythrocyte membrane by high-resolution electron microscopy. Networks were released from ghosts by extraction with Triton X-100, freed of extraneous proteins in 1.5 M NaCl, and collected by centrifugation onto a sucrose cushion. These preparations contained primarily protein bands 1 + 2 (spectrin), band 4.1, and band 5 (actin). The networks were partially disassembled by incubation at 37°C in 2 mM NaP_i (pH 7), which caused the preferential dissociation of spectrin tetramers to dimers. The fragments so generated were fractionated by gel filtration chromatography and visualized by negative staining with uranyl acetate on fenestrated carbon films. Unit complexes, which sedimented at ~40S, contained linear filaments ~7–8 nm diam from which several slender and convoluted filaments projected. The linear filaments had a mean length of 52 ± 17 nm and a serrated profile reminiscent of F-actin. They could be decorated in an arrowhead pattern with S1 fragments of muscle heavy meromyosin which, incidentally, displaced the convoluted filaments. Furthermore, the linear filaments nucleated the polymerization of rabbit muscle G-actin, predominantly but not exclusively from the fast-growing ends. On this basis, we have identified the linear filaments as F-actin; we infer that the convoluted filaments are spectrin. Spectrin molecules were usually attached to actin filaments in clusters that showed a preference for the ends of the F-actin. We also observed free globules up to 15 nm diam, usually associated with three spectrin molecules, which also nucleated actin polymerization; these may be simple junctional complexes of spectrin, actin, and band 4.1. In larger ensembles, spectrin tetramers linked actin filaments and/or globules into irregular arrays. Intact networks were an elaboration of the basic pattern manifested by the fragments. Thus, we have provided ultrastructural evidence that the submembrane skeleton is organized, as widely inferred from less direct information, into short actin filaments linked by multiple tetramers of spectrin clustered at sites of association with band 4.1.

The cytoplasmic surface of the human erythrocyte membrane is covered by a network of filamentous proteins, which remains intact after isolation in Triton X-100 (1–3). This network is durable, flexible, and elastic. It recovers the overall, long-term shape of the parent membrane after short-term deformations and stabilizes the membrane against breakdown by shear stress (4–7). Unlike the cytoskeletons of nucleated cells, this skeleton is a two-dimensional net, closely adherent to the membrane (2, 8). A variety of electron microscopic studies of the intact skeleton have revealed an irregular filamentous network with polygonal interstices 20–100 nm diam (2, 9–12).

The proteins essential to the integrity of the skeleton are bands 1 plus 2 (spectrin), band 4.1, and band 5 (actin) (3). It is thought that most of the spectrin exists in situ as ~200-nm-long, thin, and flexible filaments in the form of $(\alpha\ \beta)_2$ tetramers (13–16). The actin appears to be associated into homo-oligomers or protofilaments capable of nucleating the polymerization of rabbit muscle G-actin (11, 17–21). Spectrin tetramers have been shown to bind to and link rabbit muscle actin filaments in reconstituted systems (18, 22, 23). Such complexes are stabilized by the presence of band 4.1 (18, 24, 25), which associates in vitro near the ends of spectrin tetramers (26). The skeleton is linked to the membrane proper both by

THE JOURNAL OF CELL BIOLOGY · VOLUME 99 SEPTEMBER 1984 810–821

a second association of band 4.1, perhaps with an integral glycoprotein (27), and by the association of band 2.1 with both spectrin and band 3, the anion transporter (14, 28, 29). Spectrin, actin, band 2.1, and band 4.1 have also been detected in cytoskeleton–plasma membrane complexes in various nucleated cells (30).

Although numerous biochemical, biophysical, and ultrastructural studies over the past decade have created a broad consensus concerning the organization of this skeleton (see, for recent review, references 14, 15, and 28–33), direct visualization of its molecular architecture has been lacking. It was the goal of the present research to extend the structural analysis of the red cell skeleton by negatively staining its fragments on fenestrated carbon films.

An abstract describing this work has been published (34).

MATERIALS AND METHODS

Materials: Rat liver ribosomes and their large and small subunits, prepared (35) and generously provided by Dr. Ira G. Wool and Dr. Alan Lin, were used as sedimentation standards. Rabbit muscle F-actin, prepared according to Spudich and Watt (36), and the A1 isozyme of rabbit muscle S1 heavy meromyosin, purified chromatographically (37), were the generous gifts of Dr. Edwin W. Taylor and Dr. Steven Rosenfeld (University of Chicago). All chemicals and reagents were of analytical grade or better.

Membranes: All procedures were performed at 0–5°C, unless specified. Human erythrocytes were obtained from normal donors either fresh in Na_4 EDTA or, more frequently, from outdated units purchased from United Blood Services (Chicago, IL). The age and source of the blood had no apparent effect on our results. Ghost membranes were prepared as previously described (38) and were utilized the same day.

Skeletons: Freshly prepared ghosts (2 ml) were incubated on ice for 1 h in 8 ml of 5 mM NaP_i (pH 7) containing 2.5% (wt/vol) Triton X-100 (1). Although skeletons are labile in warm buffers of low ionic strength, they are stable at 0°C for many hours under the conditions described (5). The mixture was layered on top of a discontinuous density gradient of 10, 35, and 60% (wt/vol) sucrose in 1.5 M NaCl–5 mM NaP_i (pH 7) (3). The gradients were centrifuged at 14,000 rpm for 30 min in a Sorvall HB-4 rotor (DuPont Instruments, Sorvall Biomedical Div., Newtown, CT). The intact skeletons were collected from the 35%/60% sucrose boundary.

Preparation of Fragments: Skeletons were dialyzed against 2 mM NaP_i (pH 7) containing 0.5 mM dithiothreitol and concentrated by vacuum dialysis to ~2.0 mg/ml protein. Breakdown was induced by incubation at 37°C for various intervals (5), during which aliquots were taken and stored on ice. Approximately 8–10 mg of fragment protein was resolved by gel filtration chromatography on Fractogel TSK-HW75 (EM Science, Gibbstown, NJ) in 2 mM NaP_i (pH 7)–0.5 mM dithiothreitol in a 2.6 × 100 cm column in a cold room at a flow rate of 40 ml/h. The effluent was monitored at 280 nm and collected in 6.5-ml fractions. Selected fractions were concentrated by vacuum dialysis in a cold room for electrophoresis and electron microscopy. The column fractions were stable with respect to their electrophoretic pattern and ultrastructure both before and after concentration over a period of at least 2 wk when stored on ice in the column buffer. Protease activity present in the input ghosts and networks was absent from the column fractions.

Electrophoresis under nondenaturing conditions was carried out as in the work of Liu and Palek (4) on 0.8% agarose (Sigma Chemical Co., St. Louis, MO, type 1, low electroendosmosis) slab gels at 4°C in 50 mM Tris-glycine (pH 8.3 at 20°C) at 200 V and 15 mA for 3 h in a cold room. SDS PAGE was as described (38, 39) except that 50 mM NaP_i (pH 7.3) was the electrophoresis buffer, and the concentration of detergent was 0.1%.

Elongation of skeleton fragments was performed with monomeric G-actin generated by dialysis of rabbit muscle F-actin for 24 h in the cold room against a depolymerization buffer 2 mM Tris·HCl (pH 8.0), 1 mM dithiothreitol, 1 mM NaN_3, 0.2 mM ATP, and 0.1 mM $CaCl_2$, followed by centrifugation at 100,000 *g* for 2 h to remove residual F-actin and denatured protein. The absence of F-actin in the solution of G-actin was demonstrated by electron microscopy of negatively stained specimens.

Decoration of skeleton fragments and rabbit muscle F-actin was carried out with the S1 subunit of rabbit muscle heavy meromyosin according to the method of Moore et al. (40). Droplets of fragment suspensions were applied to fenestrated carbon films, the grids rinsed free of unadsorbed material with 0.6 M KCl, and single droplets of S1 fragments (0.1–0.35 mg/ml in 2 mM Tris·Cl, pH 8.0) applied. After 15 s at 0°C, the films were rinsed with ice-cold cytochrome *c* (0.2 mg/ml) in a 0.1% amyl alcohol solution, and the specimens examined by electron microscopy after negative staining.

Preparation of Specimens for Electron Microscopy: Fenestrated carbon films were prepared on copper grids as described (41). Single droplets of unfixed samples were allowed to adsorb to the film for 1 min on ice and the excess drawn into filter paper. The grid was then rinsed and exposed to three successive drops of an unbuffered 1% uranyl acetate solution which remained on the grid for 30 s before being drawn off. Grids were dried in room air. Glutaraldehyde-fixed specimens had a different appearance which will be described in a separate publication. Further details are provided in the individual figure legends.

Electron Microscopy: Specimens were studied in a Philips EM300 electron microscope fitted with condenser and objective apertures of 200 and 50 μm, respectively (Philips Electronic Instruments, Inc., Mahwah, NJ). The acceleration voltage was 80 kV. Microscope magnifications were calibrated with a Fullam crossed-lined grating replica (Ernest F. Fullam, Inc., Schenectady, NY). Magnifications were set after the microscope was brought to top operating magnification to minimize variance due to hysteresis of the imaging lenses. Images were recorded on Kodak electron image films and developed with full-strength Kodak D-19 developer for 5 min (Eastman Kodak Co., Rochester, NY).

The lengths of filaments were measured directly on enlarged prints with a ruler. The error of the individual measurements was never >1 mm, which corresponded to 5 nm of filament length.

RESULTS

Skeletons were prepared by extracting ghosts in Triton X-100 at low ionic strength (1) and then removing nonessential proteins and lipids by centrifugation through a sucrose barrier containing 1.5 M NaCl. As previously observed (3), the essential skeleton was composed primarily of the polypeptide bands 1, 2, 4.1, and 5 (Fig. 1, compare gels *a* and *b*). Trace amounts of band 4.9 and other minor proteins were also present but will not be discussed further.

As noted previously (1–3, 12), electron microscopy of negatively stained preparations revealed a filamentous network resembling the parent membrane in overall size and shape. There exist two limitations on the visualization of molecular details in such preparations: (*a*) the background introduced by the underlying carbon film and the thick layer of stain surrounding high local concentrations of proteins; and (*b*) the complexity of the network itself, compounded by the double layer of filaments in the collapsed structure. To overcome the former problem, we used fenestrated carbon films (41) so that the skeleton could be examined without interference from the underlying support. This type of preparation had the added advantage of generally producing a thin and relatively uniform layer of stain. To deal with the latter problem, we induced breakdown of the skeleton into fragments of convenient size.

Fragments of the Skeleton

Isolated skeletons broke down in a reproducible fashion when exposed to low ionic strength buffer at elevated temperature (5). Breakdown was primarily caused by the dissociation of spectrin tetramers to dimers (4, 42, 43); however, as shown below, some release of free spectrin, actin, and band 4.1 also occurred. Gel filtration chromatography of such preparations on columns of highly porous beads revealed four major peaks (Fig. 2). The ultraviolet absorbance profile shifted from larger to smaller fragments during the first hour but did not change much further during overnight incubation.

Each peak was analyzed by electron microscopy and gel electrophoresis under native (not shown) and denaturing conditions. Peak I was turbid and contained little protein (Fig. 1,

gel *c*); it was shown to be rich in lipid vesicles. Peak II contained primarily bands 1, 2, 4.1, and 5 (Fig. 1, gel *d*). Most of this material either did not enter or migrated very slowly on 0.8% agarose gels without denaturation, suggesting complexes substantially larger than spectrin tetramers (which have a molecular weight of ~10^6). Peak II material sedimented at ~40S–100S upon rate zonal centrifugation on sucrose gradients. Peak III was rich in both complexed and uncomplexed spectrin but contained bands 4.1 and 5 as well (Fig. 1, gel *e*). Peak IV contained both spectrin and actin but was enriched in the latter compared to the input (Fig. 1, gel *f*). The spectrin appeared to be in the form of dimers by both electron microscopy and nondenaturing gel electrophoresis. No actin filaments were observed in peak IV material.

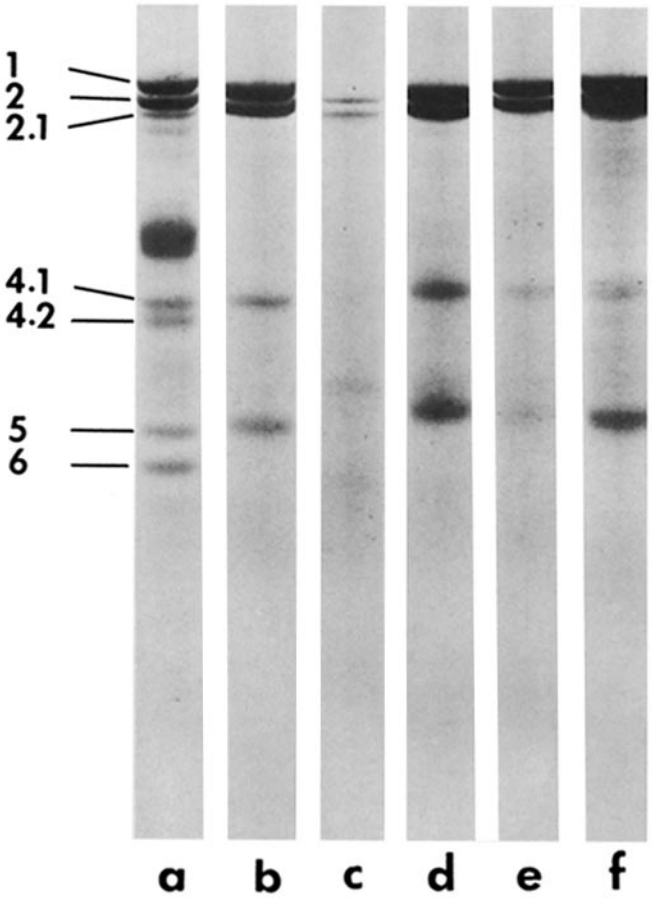

FIGURE 1 Electrophoretic profile of the polypeptides of ghosts, skeletons, and chromatographic fractions. Skeletons were prepared from purified ghosts and incubated for 30 min at 37°C in 2 mM NaP_i (pH 7.0) and the fragments were chromatographed (see Fig. 2). Peak fractions were concentrated for electron microscopy (see Fig. 3) and gel electrophoresis in SDS. (a) Intact ghosts; (*b*) intact skeletons; (c) peak I, fraction 31; (*d*) peak II, fraction 37; (e) peak III, fraction 47; (*f*) peak IV, fraction 52.

Microscopically, the predominant forms in peak II were linear filaments with a thickness of ~7–8 nm to which multiple, thin, convoluted filaments were attached (Fig. 3). The more excluded fractions contained the largest complexes. These structures remained stable (after the initial breakdown) during overnight incubation at 37°C. The linear filaments had a serrated profile, suggesting a helical structure. The data presented below establish that the linear filaments are actin and the thin, convoluted filaments spectrin.

The spectrin filaments were usually clustered at intervals along and at both ends of the actin filaments (Fig. 3), suggesting discrete, polyvalent attachment sites or cooperative rather than random binding. Thickening of the linear filaments was sometimes observed at these junctions. Most of the spectrin molecules in peak II were attached by one end to an actin filament, presumably because they had been dissociated to monovalent dimers during the low ionic strength incubation (41, 42). However, in material from the more excluded fractions of the elution profile, two or more actin filaments were often linked by one or more spectrin filament (Fig. 3, lower panels).

The length of the actin filaments in peak II fragments is plotted in Fig. 4. After recording the data, we reexamined the longest structures (i.e., >100 nm) and concluded that they were probably composed of two or three short actin filaments linked by spectrin. By neglecting the longest 17 out of 445 structures, we found that their size distribution was nearly Gaussian; that is, unimodal with similar values for the mean (52 nm), median (51 nm), and mode (51 nm). The standard deviation of the mean was 17 nm. As suggested by the fit of the data to a Gaussian curve (Fig. 4), we may have undercounted the shortest filaments (<20 nm), both because their identification was difficult and because they may have migrated in peak III rather than peak II.

Peak III contained free spectrin as well as circular figures (globules or disks) up to 15 nm diam, often associated with three spectrin filaments (Fig. 5). The arrangement of spectrin around the globules sometimes resembled triskelions, a form characteristic of clathrin (44) and also recently noted in fragments of the erythrocyte skeleton (45).

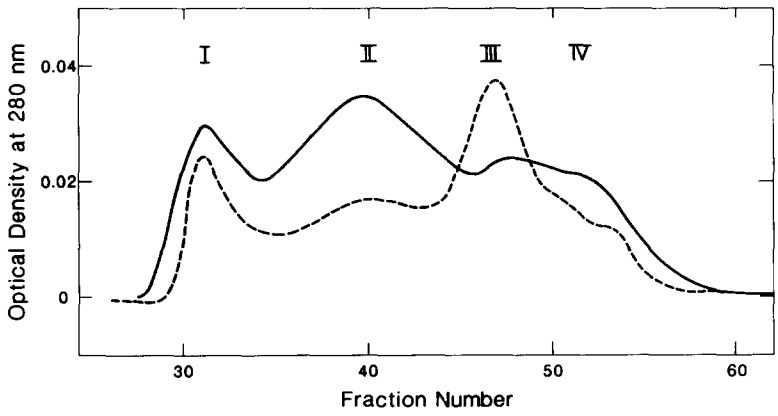

FIGURE 2 Chromatographic profile of skeleton fragments. Skeletons from 8 ml of ghosts were incubated in 2 mM NaP_i (pH 7.0) for either 30 min (solid line) or 45 min (dashed line). Approximately 8 mg of protein in 5 ml was chromatographed on a Fractogel column (see Materials and Methods) and optical absorbance was monitored at 280 nm.

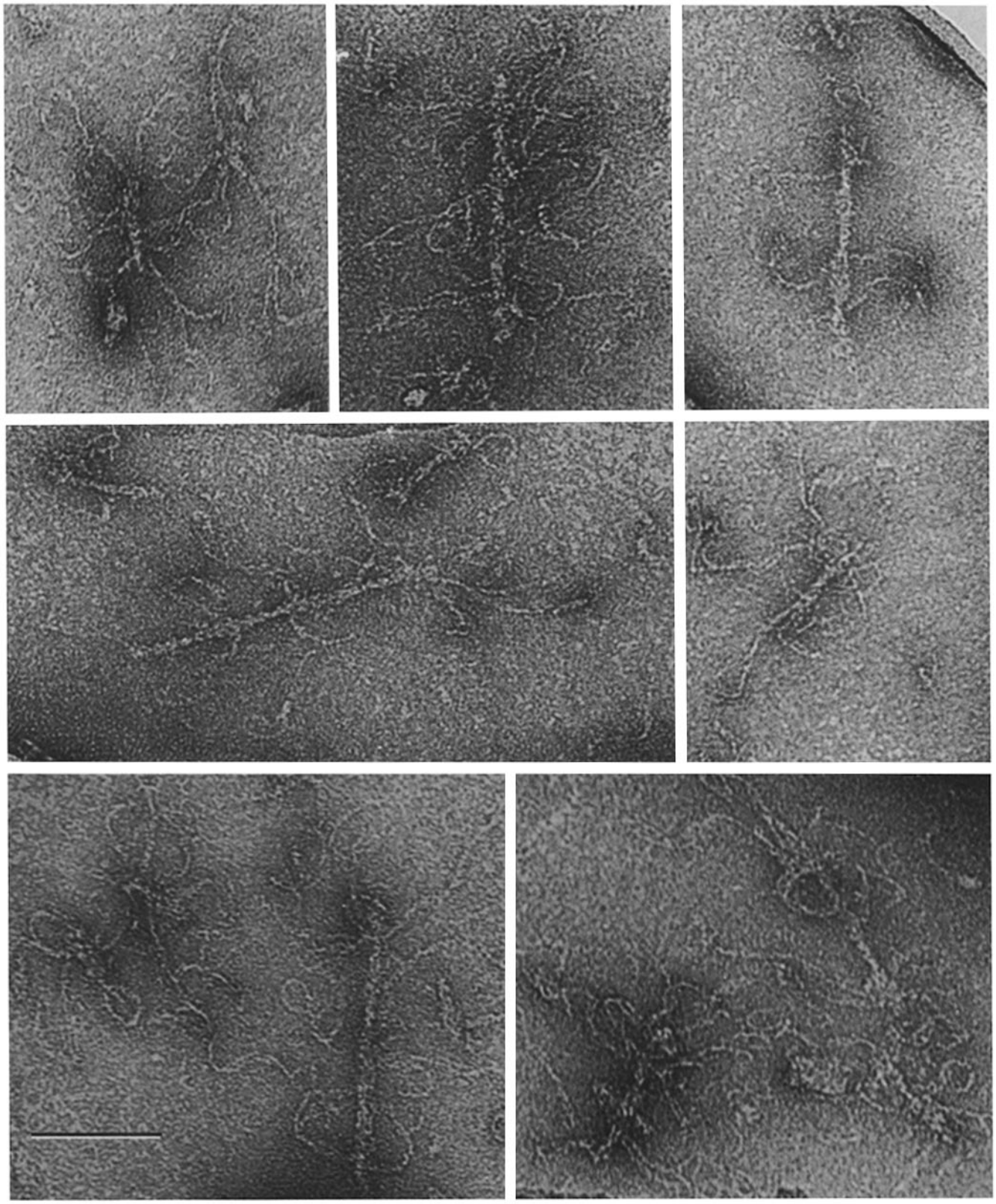

FIGURE 3 Peak II fragments. Fractions 36–38 from the 30-min sample in Fig. 2 were pooled, concentrated, and prepared for electron microscopy as described in Materials and Methods. The fragments were typically linear filaments, which we assumed to be actin, to which several convoluted filaments, which we assumed to be spectrin, were associated in clusters. Note the thickening of some of the junctions of spectrin and actin and the tendency of these junctions to occur at the ends of the actin filaments. Note also that the lower set of panels contained multiple protofilaments of actin linked by spectrin. Bar, 50 nm.

The length of spectrin filaments in peaks II and III was difficult to determine because of their convoluted contour, overlapping pattern, and nonuniform staining. Many could not be traced for >10–20 nm. Conceivably, they are serpentine and may be only partially embedded in the very thin layer of stain (cf. reference 46). In addition, we consider that breakage of spectrin molecules may have occurred under the conditions used for their visualization. A similar observation has been made with rotary shadowing (23). The stoichiometry of spectrin on actin filaments was likewise difficult to ascertain and might be underestimated, in any case, given the partial release of spectrin from the complexes.

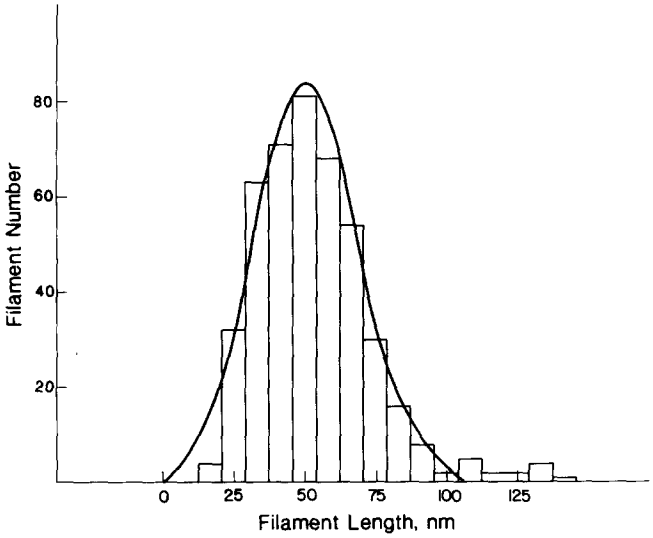

FIGURE 4 Length of actin filaments. Specimens from the peak II region of several experiments comparable to that shown in Figs. 1–3 were photographed and the length of the 7–8-nm-diam linear filaments was measured. The solid line represents a Gaussian curve calculated from the measured mean and standard deviation of the data for filaments <100 nm long.

Identification of Actin Protofilaments

The thickness, linearity, and helical substructure of the linear filaments suggested that they were oligomers of actin. Two tests of this premise were performed. First, an excess of monomeric rabbit muscle G-actin was incubated with material from peak II under conditions, which did not allow nucleation of F-actin in control experiments lacking network fragments. As illustrated in Fig. 6, essentially all of the linear filaments in the fragments became indefinitely extended (i.e., micrometers in length) through the accretion of G-actin. It is important to note that the associated spectrin was usually clustered at or near one end of the actin filaments (panels *a* and *b*). This disposition makes it clear that the skeleton fragments remained stable and were able to nucleate polymerization. Only one end of the protofilaments was significantly extended by exogenous G-actin; the other end was either not demonstrably elongated or was extended <50 nm from the spectrin complex (i.e. <5% of the rapidly growing end). When we used a high ratio of fragments to G-actin, spectrin clusters were also observed in the middle of the filaments, presumably reflecting polymerization and annealing at both ends of red cell actin oligomers (47).

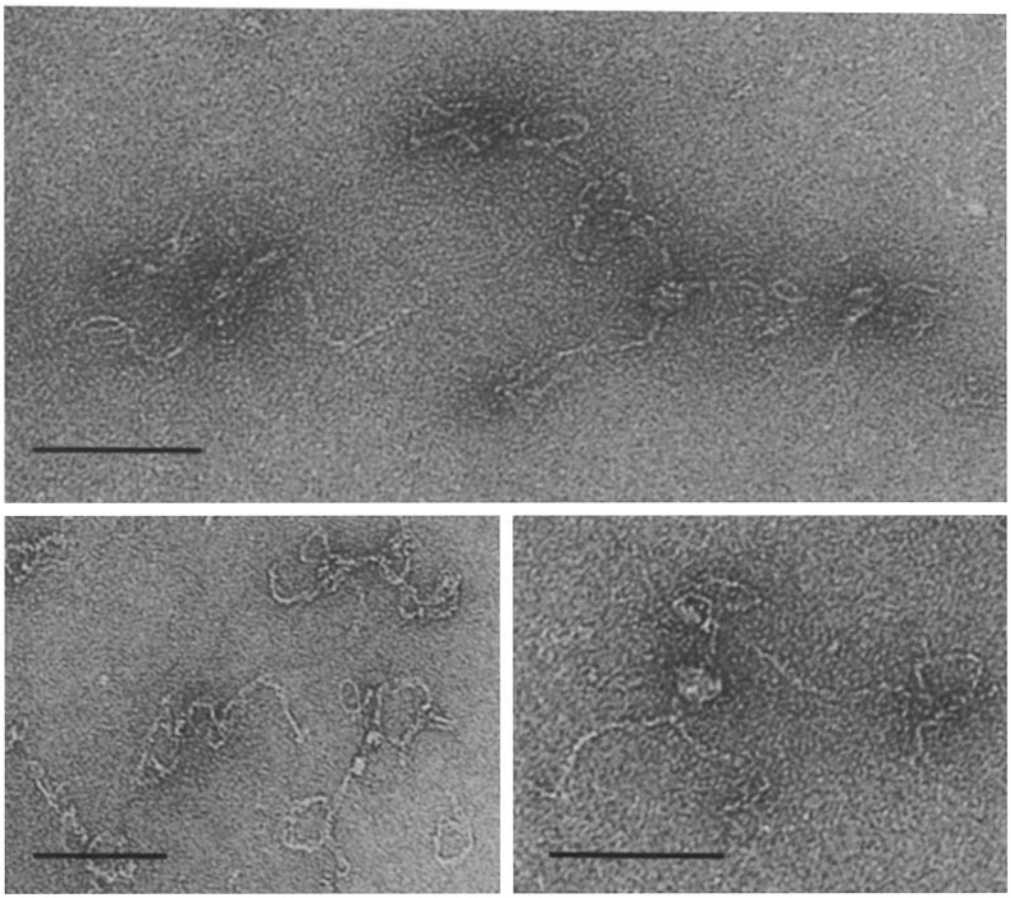

FIGURE 5 Peak III fragments. Skeletons from 8 ml of ghosts were incubated in 2 mM NaP_i (pH 7.0) for 3 h. Approximately 5.5 mg of protein in 4 ml was chromatographed as in Fig. 2. Fraction 47 was concentrated and prepared for electron microscopy as described in Materials and Methods. These fragments were typically globules or disks up to 15 nm diam either free or associated with up to three spectrin molecules, often arranged as triskelions. Bar, 50 nm.

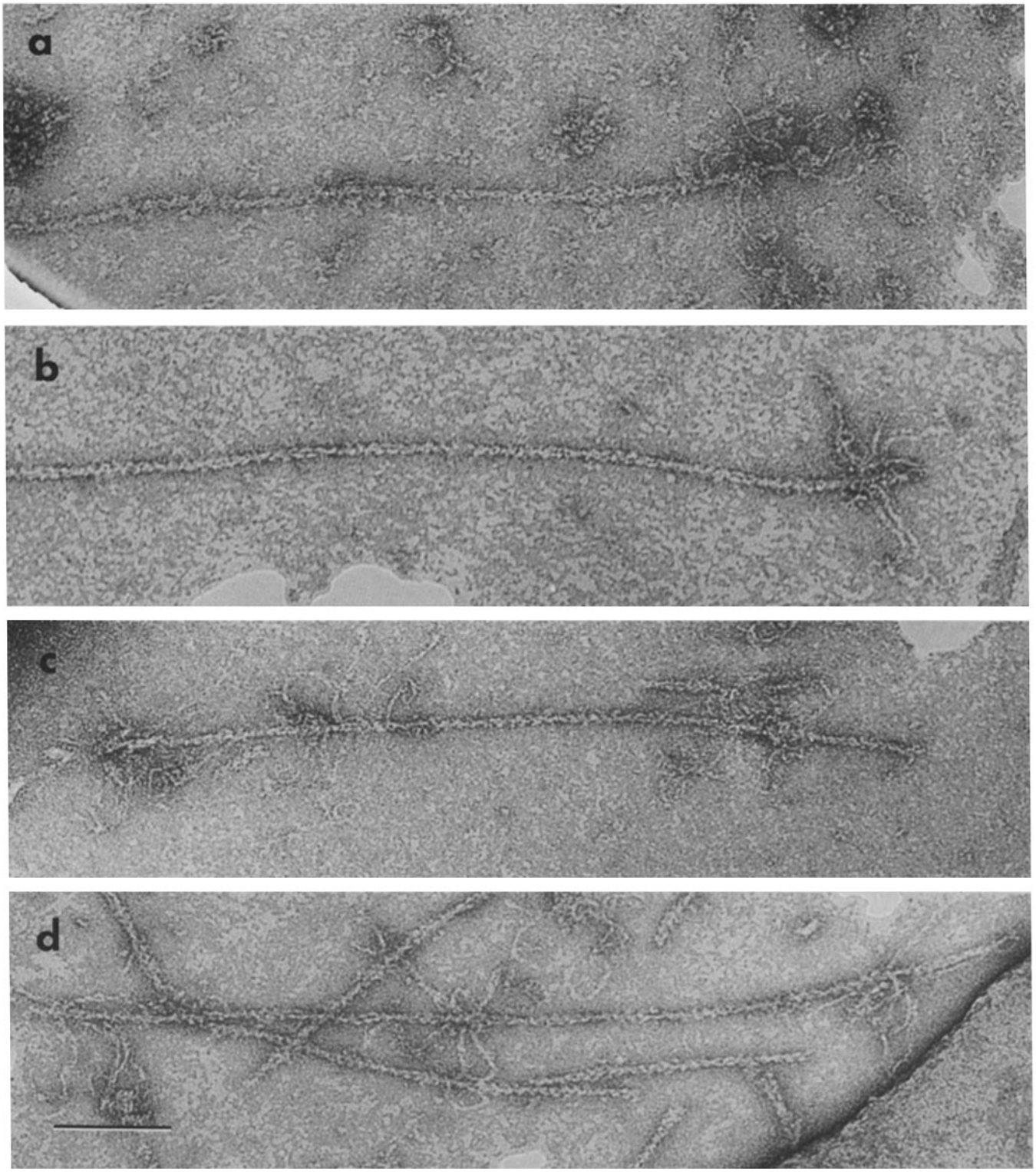

FIGURE 6 Elongation of peak II fragments with G-actin. Preparations of peak II fragments in 200 μl were brought to ~50 mM NaCl–3 mM NaP_i (pH 7) and incubated with 20 μl of G-actin (prepared in the depolymerization buffer described in Materials and Methods) for 10 min at room temperature. (*a* and *b*) The incubation mixture contained ~30 μg/ml of peak II protein and 66 μg/ml of G-actin; (*c* and *d*) the incubation mixture contained ~104 μg/ml of peak II protein and 64 μg/ml of G-actin (final concentrations). The reactions were stopped by the addition of an equal volume of ice-cold buffer (0.15 M NaCl–5 mM NaP_i, pH 7). The specimens were examined by electron microscopy as described in Materials and Methods. Control experiments lacking peak II fragments but containing G-actin at twice the concentration stated above showed no actin polymerization. Bar, 50 nm.

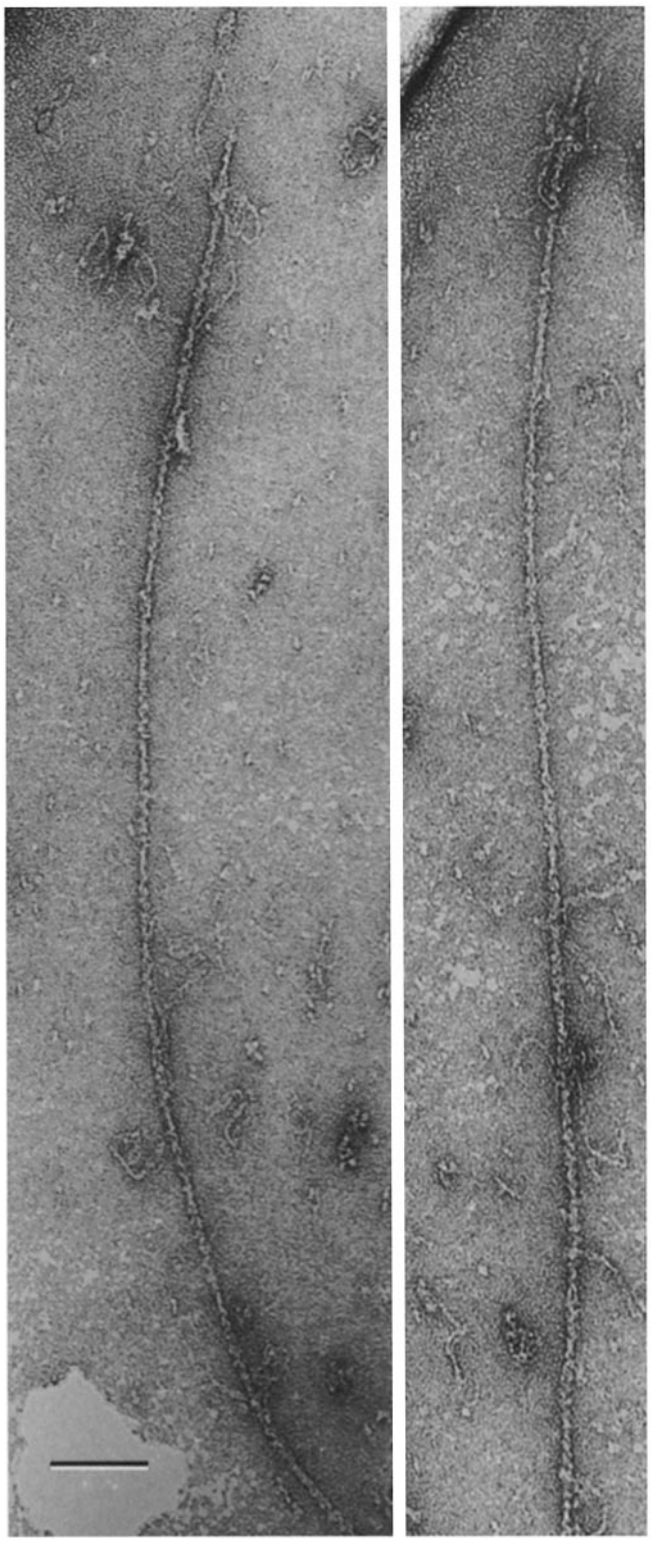

FIGURE 7 Elongation of peak III fragments with G-actin. Preparations of peak III fragments in 200 μl were brought to ~50 mM NaCl–3 mM NaP_i (pH 7) and incubated with 25 μl of G-actin (prepared in the depolymerizing buffer described in Materials and Methods) for 10 min at room temperature. The final concentrations of peak III protein and G-actin in the incubation mixture were 44 and 78 μg/ml, respectively. The reaction was stopped by the addition of an equal volume of ice-cold buffer (0.15 M NaCl–5 mM NaP_i, pH 7). The specimens were examined by electron microscopy as described in Materials and Methods. Control experiments lacking peak III fragments but containing G-actin at twice the concentration stated above showed no actin polymerization. Bar, 50 nm.

The globules obtained from peak III also nucleated the polymerization of rabbit muscle G-actin (Fig. 7). Sometimes elongation propagated in both directions, but one end always greatly predominated. Free spectrin molecules present in these preparations occasionally adhered to the actin filaments, as previously observed in reconstituted systems (18, 22, 23).

A second test for actin oligomers was to decorate skeleton fragments with the S1 fragment of heavy meromyosin (40). The long structure in the top panel of Fig. 8 shows, for reference, a filament of rabbit muscle actin decorated in this fashion to reveal the diagnostic repeating arrowhead pattern. Fragments from red cell skeletons showed comparable decoration (Fig. 8, lower panel). Note that, under the conditions of this experiment, the S1 fragments completely displaced the spectrin filaments that were present in the untreated fragments (as in Fig. 3).

The accretion of G-actin on S1-decorated muscle F-actin is more rapid at the barbed than pointed end of the arrowhead pattern (40, 48). We tested whether red cell actin shared this property. Fragments of the network were first elongated by the addition of a small amount of monomeric actin and then decorated with the S1 portion of heavy meromyosin. The bound spectrin served as a marker for the locus of the red cell actin in the extended F-actin. Although the S1 fragments caused some displacement of spectrin, we observed that the arrowhead pattern pointed invariably to the end of the actin filaments which bore the residual spectrin (Fig. 9). Thus, accretion of globular actin occurred predominantly at the barbed ends of the red cell actin oligomers just as in the case of muscle actin.

Unfragmented Skeletons

We extended our study to the fine structure of the unfragmented skeleton, which was spread on fenestrated carbon films. Intact skeletons were difficult to study because the double layer of filaments was so dense. We found that the upper layer of the skeleton could be stripped away from the layer adherent to the carbon film by repeated washing with deionized water or unbuffered 1% uranyl acetate (but not with saline). Some elements in the adherent portion of the skeleton were also extracted in this procedure, but most of the structure remained intact and well resolved after this clearing step. (We noted that the water and uranyl acetate extraction was effective only in the fenestrated regions of the grid. Elements of both layers of the skeleton in direct contact with the carbon film were not removed, presumably because of their strong adsorption to the support, as is also the case on unfenestrated films.) Interpretation of the structure of the network was also made difficult by the inherent complexity of the reticular pattern. For example, it was not always possible to distinguish sites of filament association from overlapping structures or to distinguish clusters of spectrin from actin filaments.

Two micrographs representing extremes of variation observed in our preparations are presented in Fig. 10. These images resemble earlier results with negative staining (11, 12); however, our study seems to have benefited greatly from the use of fenestrated supports. The skeletons appeared to be an elaboration of the basic pattern of the fragments. That is, linear filaments of actin as well as globules of up to 15 nm in diam were linked by multiple filaments of spectrin. Spectrin filaments often appeared to arise in clusters from sites distributed irregularly along the actin filaments. Sometimes, spectrin

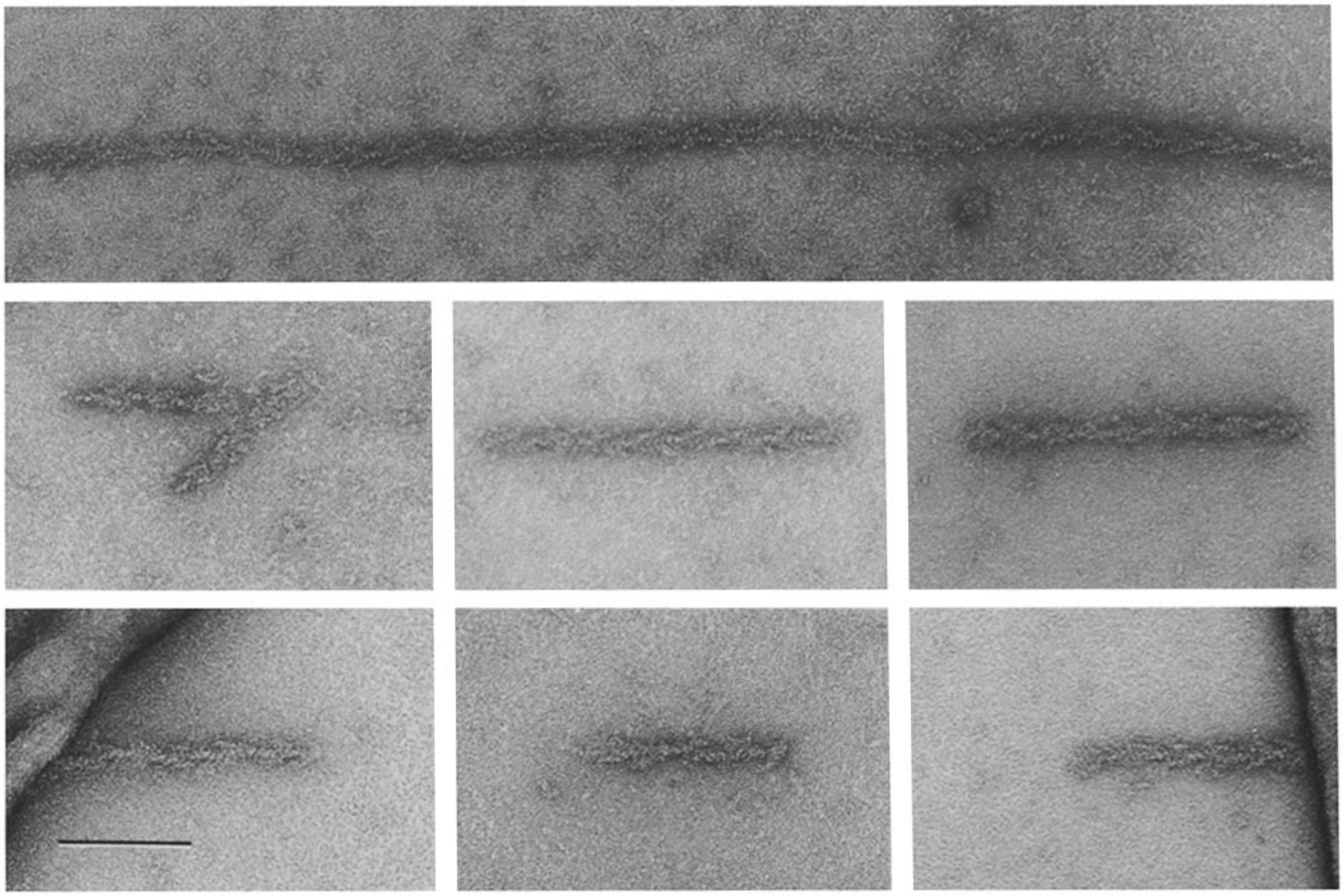

FIGURE 8 Decoration of peak II fragments. Preparations of rabbit muscle F-actin (1 mg/ml; *top*) and peak II fragments (30 μg/ml; *bottom*) were applied to fenestrated carbon films and decorated with S1 fragments of heavy meromyosin (350 μg/ml) as described in Materials and Methods. Bar, 50 nm.

molecules ran in parallel array between neighboring actin protofilaments. The spectrin was more elongated and less convoluted in the skeletons than the isolated fragments, presumably a manifestation of both the spreading forces created by the adherence of the networks to the carbon film and the two-point attachment of spectrin tetramers to actin filaments. Some spectrin filaments measured ~200 nm, the length of the isolated spectrin tetramer (13). The length of the actin filaments corresponded to those in the fragments. Actin protofilaments could be elongated in situ by the addition of G-actin (not shown).

Some areas of the skeleton took the form of patches of dense reticulum too complex for analysis (Fig. 10*a*). These could arise from a high degree of connectivity and interweaving among a limited number of spectrin and actin filaments. Presumably, breaking some connections would turn these tightly woven mats into more extended arrays.

DISCUSSION

We have induced the fragmentation of isolated red cell membrane skeletons, separated the fragments according to size and analyzed their structure by electron microscopy. In discussing our results, we have adopted the following terms, illustrated in Fig. 11. The basic skeleton, which contains only those proteins essential to its integrity, is an irregular two-dimensional reticulum compounded of spectrin, actin, and band 4.1. We shall call the structures remaining when all spectrin molecules are reduced to dimers and no other bonds are broken unit complexes (akin to the "unit cells" of Cohen; [32]). Junctions are the linkage sites of spectrin, actin, and band 4.1 (11). There are also regions of uncomplexed F-actin.

Breakdown of the skeleton at low ionic strength (typically, $\mu = 0.001$–0.010) appears to occur at three loci: between spectrin dimers, between actin monomers, and at the junction of spectrin, actin, and band 4.1 (see Fig. 11). Spectrin tetramers dissociate to dimers within minutes in low ionic strength buffer at 37°C (4, 17, 42, 43). The junctions are also quite labile under these conditions in ghosts but, for unknown reasons, are rather stable when isolated in Triton X-100 (5). Unit complexes were generated by warming isolated skeletons at low ionic strength, thus preserving junctions while dissociating most spectrin tetramers to dimers. Those spectrin tetramers that remained demonstrated the ensemble structure of the network. The presence of dissociated spectrin and actin in peaks III and IV indicated, however, that some breakdown of junctions also occurred during the incubation. Nevertheless, the similarity of the organization of the isolated complexes and the intact skeletons suggests that the fundamental pattern of associations was not altered by fragmentation. We are currently evaluating the ultrastructure of the skeleton maintained exclusively in physiologic buffers.

Incubation of ghosts at low ionic strength in the absence of detergent has also been found to liberate high molecular weight complexes of spectrin, actin and band 4.1 (4, 17, 18, 24, 42). Those complexes may correspond to our fragments.

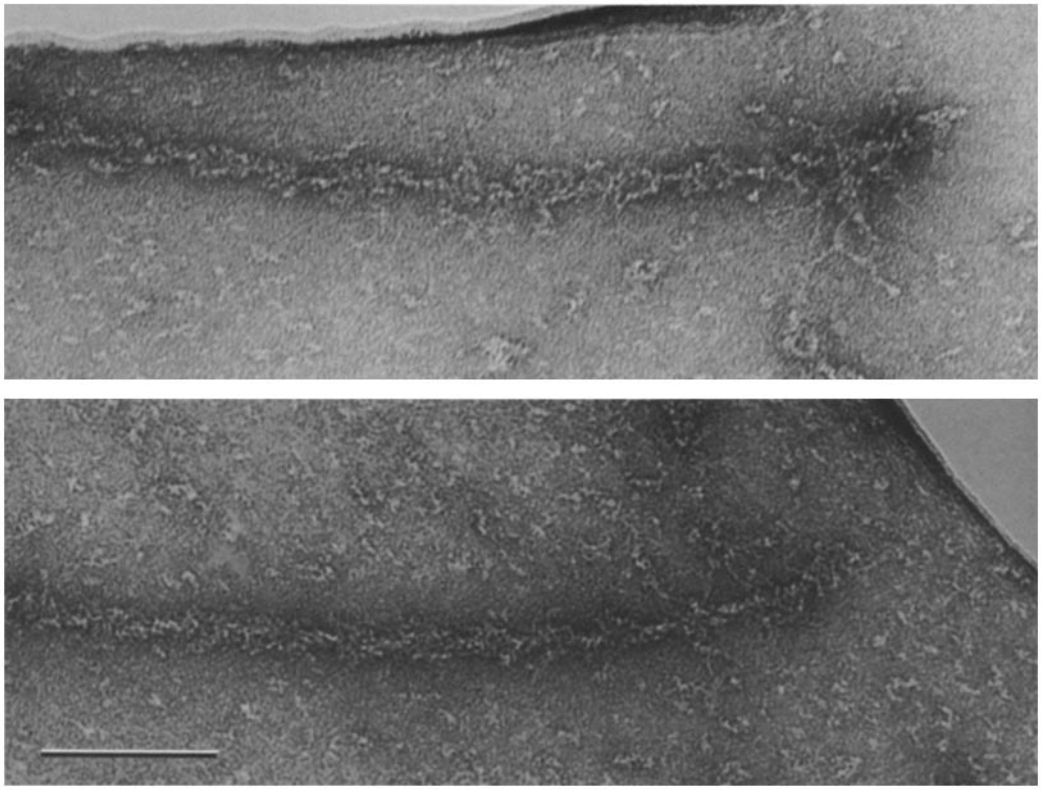

FIGURE 9 A test of the polarity of peak II fragment protofilaments. Preparations of peak II fragments were elongated as part of the experiment shown in Fig. 6, *c* and *d*, applied to fenestrated carbon films, and decorated with S1 fragments of heavy meromyosin (350 μg/ml) as described in Materials and Methods. The rapidly growing end of the erythrocyte actin was invariably barbed. Bar, 50 nm.

However, their solubilization required the dissociation of band 4.1 from the membrane, to which it is usually firmly bound at low ionic strength (38). Furthermore, the high molecular weight complexes comprised a small and variable fraction of those extracts and may not have been representative of the whole. It seemed to us, therefore, that fragments generated from skeletons isolated in Triton X-100 were more likely to reveal native organization than the complexes obtained directly from ghosts.

The fragments generated in our study included the following: free spectrin dimers and tetramers, G-actin, and band 4.1; free globules bearing up to three dimers of spectrin; actin filaments associated with spectrin dimers; globules and protofilaments linked by one or more spectrin tetramers; and larger complexes built upon these units. We did not observe either large spectrin oligomers lacking actin (45, 49) or actin bundles (50). It is unlikely that our experiments induced unphysiologic associations, since (*a*) the low ionic strength buffers we employed are known to promote only dissociation of spectrin, actin, and band 4.1 ensembles; (*b*) free monomeric units of spectrin, actin, and band 4.1 were generated rather than consumed during the incubations, suggesting progress toward a dissociated equilibrium state rather than association; (*c*) the unfragmented skeletons were discrete bodies of the approximately size and shape of the parent membranes rather than aggregates or precipitates expected from associations induced in vitro; and (*d*) the ultrastructure of the fragments was entirely consistent with that in the unfragmented skeletons.

Although there is now substantial evidence for oligomeric actin in the erythrocyte membrane (17–21), this study presents the first visual demonstration of F-actin within the native skeleton. Our estimate of the number-average actin filament length, 52 nm, corresponds to 19 protomers of actin, assuming 2.73 nm per actin (51). This value is at the upper end of the range determined by cytochalasin binding: 10–18 actin protomers (17, 19, 21) suggesting an average filament length of 27–50 nm. The smallest oligomers may have been undercounted in our study, particularly because we did not include the free 15-nm globules, which could contain polymers of up to six actin monomers. Despite the agreement between our estimate of actin size and that inferred from the binding of cytochalasin, our buffer conditions could have promoted the erosion of unprotected actin from the ends of the protofilaments. We are currently examining preparations protected against such breakdown. Atkinson et al. (20) have purified F-actin from ghosts extracted at low ionic strength in the presence of phalloidin by digesting away spectrin and band 4.1. The filaments they observed were quite long and their distribution skewed to the right; the longest filaments were 900 nm, the mean was 212 nm, the median was 146 nm, and the mode was 90 nm. Phalloidin may not merely have stabilized F-actin but may have induced the growth of long filaments at the expense of the short filaments and G-actin present in those extracts (52).

Our experiments demonstrate that erythrocyte actin in both the protofilaments and the globules is capable of extension from both ends. As is true of muscle F-actin, the barbed end of S1-decorated erythrocyte actin grew much faster than the pointed end. Our results differ from those of Pinder and Gratzer (21), who previously concluded that the pointed end is completely blocked because cytochalasin E abolished the

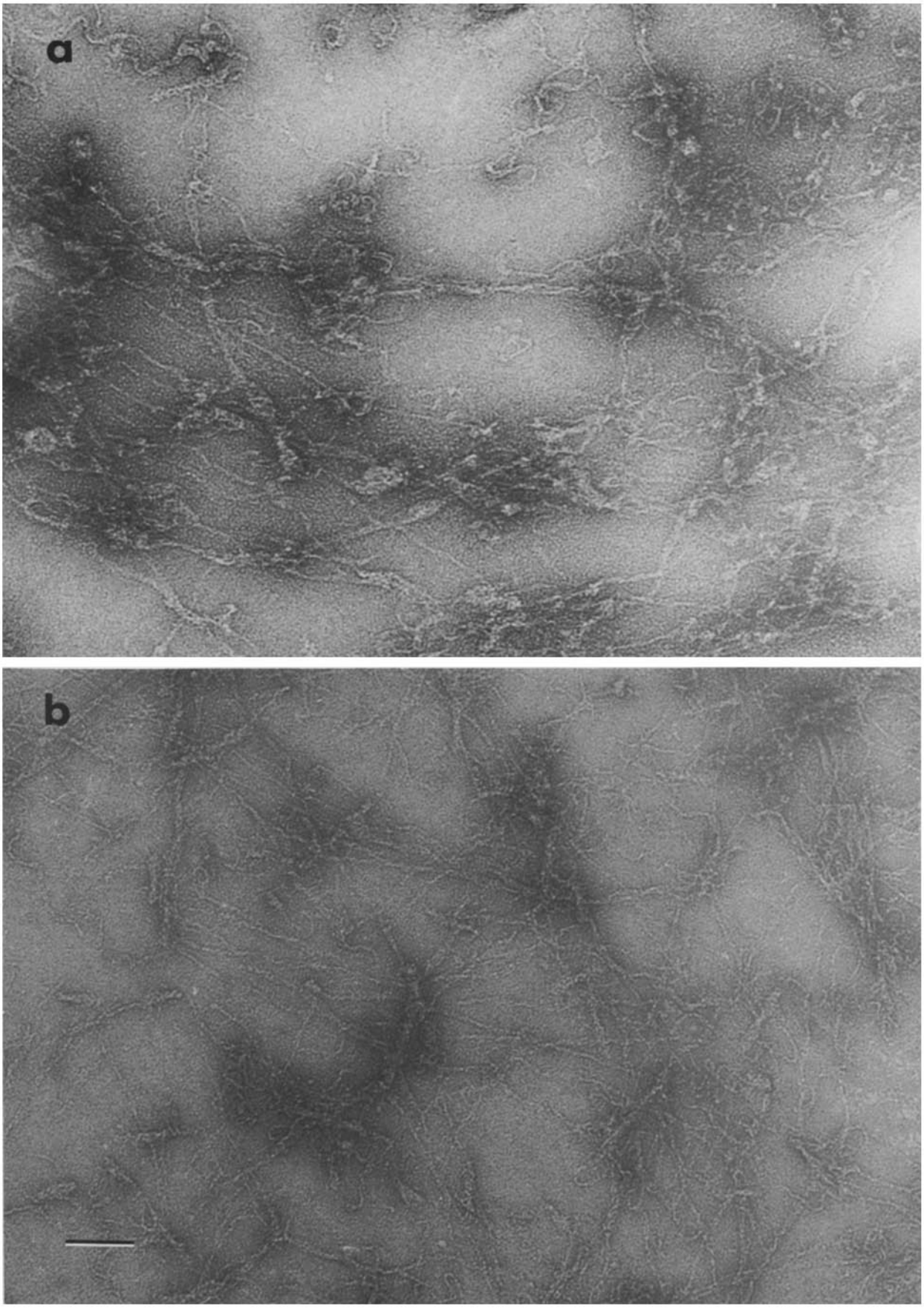

FIGURE 10 The unfragmented skeleton. Skeletons from two different preparations were dialyzed against 2 mM NaP_i (pH 7)–0.5 mM dithiothreitol applied to fenestrated films at a concentration of ~350 μg protein/ml, and stained as described in Materials and Methods. Bar, 50 nm.

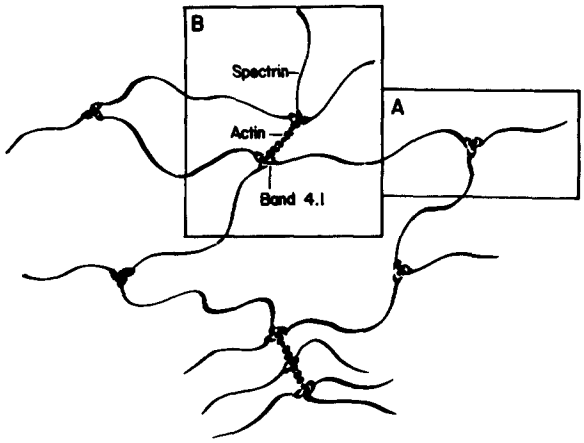

FIGURE 11 A schematic diagram of the human erythrocyte membrane skeleton. This diagram is intended to illustrate the following working hypothesis: the network is built of actin protofilaments linked by spectrin tetramers. Oligomers of band 4.1 stabilize the association of spectrin and actin in clusters called junctional complexes. Some actin protofilaments are short (perhaps three to six monomers) and do not extend beyond the globular junctional complex (as in box *A*). Other junctional complexes reside at the ends of and within longer actin protofilaments (as in box *B*). Unit complexes (e.g., those circumscribed by boxes *A* and *B*) can be liberated by warming isolated skeletons at low ionic strength which dissociates spectrin tetramers to dimers. Unit complexes may remain coupled to a varying extent through residual bivalent tetramers of spectrin.

uptake of fluorescently labeled rabbit muscle G-actin in their ghost preparations. Likewise, Cohen and Branton (53) found that the polymerizing of actin on inside-out erythrocyte membrane vesicles generated filaments whose pointed ends faced the membrane exclusively. It could be that our isolates have been partially depleted of a factor which normally inhibits growth at the pointed end, as suggested (21). Alternatively, the conditions used here may have allowed bidirectional growth. Specifically, the experiments of Pinder and Gratzer (21) employed G-actin below its critical concentration for accretion at the slow (pointed) ends of F-actin (54, 55). Because growth at the pointed ends of F-actin can sometimes be negligible even at G-actin levels exceeding the critical concentration (48), the absence of polymerization at that end may not be impelling evidence for a blocking protein. Finally, independent evidence for our hypothesis that erythrocyte membrane actin is free to polymerize at both ends has just been published (56).

The globules shown in Fig. 5 appear to be junctional complexes in three respects: (*a*) They bind spectrin. (*b*) They nucleate the polymerization of G-actin (Fig. 7). (*c*) They bear a resemblance to the globular masses created by Cohen et al. (23) from dimeric spectrin, band 4.1, and rabbit muscle G-actin. Since similar globules and nodes have been observed in intact skeletons in Fig. 10 and by others (2, 11, 12), there is reason to consider them physiologic and not artifactual. However, an undetermined number of free globules may have been released from actin protofilaments that disintegrated in low ionic strength buffer.

Although not directly visualized, it is quite likely that band 4.1 is present in the junctions of spectrin and actin seen in Figs. 3, 4, and 10. The clustering of spectrin filaments at intervals along the actin protofilament may therefore be attributable to polyvalent complexes of band 4.1 molecules (see also reference 21), given the evidence for oligmerization of purified band 4.1 (26, 57). Similar clusters of spectrin on actin filaments were observed by Cohen et al. (23) when the purified proteins were recombined in the presence of band 4.1. As in our fragments, free junctions were globular whereas junctions incorporated into F-actin were, at best, only slightly thickened (23).

The actin protofilaments in Fig. 3 might have been stabilized against erosion by junctional complexes at their ends, since neither phalloidin, Mg^{++}, nor ATP was required for their preservation even during prolonged incubation at 37°C in low ionic strength buffer. Our data thus support the hypothesis that the failure of human erythrocyte F-actin to depolymerize significantly upon equilibration of complexes at high dilution (11, 21), at low ionic strength (57), or in the presence of deoxyribonuclease I (11, 21, 58) reflects its sequestration both within and between junctional complexes (see also reference 19). However, the ability of junctional complexes to inhibit depolymerization of the actin protofilaments in vitro clearly does not prevent their elongation.

While junctional complexes may stabilize the actin filaments and confer a minimal length of 15 nm, there is no evidence that they impose a unit length. Rather, the observed Gaussian distribution of actin filament lengths suggests that the junctions are randomly incorporated into actin filaments. Uncomplexed F-actin could become sequestered between junctional complexes during erythrocyte maturation and thereafter prevented from depolymerizing except after rupture of the actin filament. It remains to be established, however, whether junctional complexes have a preference for the very ends of actin filaments in vivo or whether this pattern is a consequence of actin erosion at low ionic strength in vitro.

Tropomyosin recently has been identified in human erythrocytes prepared in the presence of magnesium (59). Tropomyosin from muscle and nonmuscle cells typically binds to F-actin with periodicities of 38.5 nm and 33–34 nm, respectively (60, 61). This suggests that pairs of tropomyosin molecules in register could span 12–14 monomers of actin in the erythrocyte. If actin protofilaments of this size were capped at each end by complexes of spectrin and band 4.1 unit lengths of the size observed here (19 actin monomers) might be generated. The broad Gaussian distribution demonstrated in Fig. 4 could reflect disproportionation of actin monomers following the loss of tropomyosin and destabilization of spectrin–band 4.1 complexes during the isolation of the skeletons. Since tropomyosin appears to compete with spectrin for association with F-actin (62), our observation of spectrin binding along the length of actin protofilaments could similarly reflect rearrangements following isolation. We are currently evaluating these hypothesis by measuring the size of actin protofilaments and the pattern of spectrin binding to actin in skeletons from which the tropomyosin has not been removed.

Our results bear on the stoichiometry of the proteins within unit complexes. Overall, the membrane contains approximately one spectrin dimer and one band 4.1 for every 2.5 actin monomers (21). If a spectrin–band 4.1 complex required two actin monomers for proper binding, only 20% of the total actin would be uncomplexed and 80% would be contained within junctional complexes. However, if the spectrin dimer–band 4.1-actin monomer complex had a 1:1:1 stoichiometry, as recently suggested (63), 60% of the actin would be uncomplexed and would presumably flank the junctional complexes containing the remaining 40% of the actin. The latter alternative is supported by our data (Fig. 3). One can readily calculate from the stoichiometry determined in Pinder and

Gratzer (21) that the average protofilament of 20 actin subunits would bear eight spectrin–band 4.1 complexes. Given the pattern of three spectrins per globule (Fig. 5) and the preference of the junctional complexes for both ends of the protofilaments (Fig. 3), a typical unit complex might have six spectrins associated with its ends and two spectrins clustered somewhere in the middle. Smaller actin oligomers might merely have junctions at their ends while long protofilaments would have several internal junctions. This idealized view is consistent with our data (Figs. 3 and 10).

In conclusion, our observations confirm the working hypothesis concerning the molecular organization of the erythrocyte skeleton currently embraced by most students of the subject (14, 15, 23, 28–33). Furthermore, the study of fragments provides ultrastructural details available from neither the isolated and reconstituted proteins nor from the intact skeleton itself.

The authors thank Peter Nyguen and Albert Sorrell for their excellent technical assistance in this study.

This work was supported by American Heart Association grant 81-664 (BWS), American Cancer Society grant BC-95 (TLS), and National Institutes of Health grants HLI 22654 (RJ) and HL 30121. Betty W. Shen is an Established Investigator of the American Heart Association (grant 79-131) and Robert Josephs was the recipient of an National Institutes of Health Research Career Development Award (grant HL 00434).

Received for publication 30 January 1984, and in revised form 14 May 1984.

REFERENCES

1. Yu, J., D. A. Fischman, and T. L. Steck. 1973. Selective solubilization of proteins and phospholipids from red blood cell membranes by nonionic detergents. *J. Supramol. Struct.* 1:233–248.
2. Hainfeld, J., and T. L. Steck. 1977. The sub-membrane reticulum of the human erythrocyte: a scanning electron microscopic study. *J. Supramol. Struct.* 6:301–317.
3. Sheetz, M. P. 1979. Integral membrane protein interaction with triton cytoskeletons of erythrocytes. *Biochim. Biophys. Acta* 557:122–134.
4. Liu, S. C., and J. Palek. 1980. Spectrin tetramer-dimer equilibrium and the stability of erythrocyte membrane skeletons. *Nature (Lond.).* 285:586–588.
5. Lange, Y., R. A. Hadesman, and T. L. Steck. 1982. Role of the reticulum in the stability and shape of the isolated human erythrocyte membrane. *J. Cell Biol.* 92:714–721.
6. Palek, J., and S. E. Lux. 1983. Red cell membrane skeletal defects in hereditary and acquired hemolytic anemias. *Semin. Hematol.* 20:189–224.
7. Mohandas, N., J. A. Chasis, and S. B. Shohet. 1983. The influence of membrane skeleton on red cell deformability, membrane material properties, and shape. *Semin. Hematol.* 20:225–242.
8. Nicolson, G. L., V. T. Marchesi, and S. J. Singer. 1971. Localization of spectrin on the inner surface of human red blood cell membranes by ferritin-conjugated antibodies. *J. Cell Biol.* 51:265–272.
9. Tsukita, S., S. Tsukita, and H. Ishikawa. 1980. Cytoskeletal network underlying the human erythrocyte membrane. Thin section electron microscopy. *J. Cell Biol.* 85:567–576.
10. Nermut, M. V. 1981. Visualization of the "membrane skeleton" in human erythrocytes by freeze-etching. *Eur. J. Cell Biol.* 25:265–271.
11. Pinder, J. E., S. E. Clark, A. J. Baines, E. Morris, and W. B. Gratzer. 1981. The construction of the red cell cytoskeleton. *In* The Red Cell: Fifth Ann Arbor Conference. G. J. Brewer, editor. Alan R. Liss, New York. 343–354.
12. Rimme, A. H. 1981. The ultrastructure of the erythrocyte cytoskeleton at neutral and reduced pH. *J. Ultrastruct. Res.* 77:199–209.
13. Shotton, M. D., B. E. Burke, and D. Branton. 1979. The molecular structure of human erythrocyte spectrin. Biophysical and electron microscopic studies. *J. Mol. Biol.* 131:303–329.
14. Branton, D., C. M. Cohen, and J. Tyler. 1981. Interaction of cytoskeletal proteins on the human erythrocyte membrane. *Cell.* 24:24–32.
15. Marchesi, V. T. 1979. Spectrin: present status of a putative cyto-skeletal protein of the red cell membrane. *J. Membr. Biol.* 51:101–131.
16. Marchesi, V. T. 1983. The red cell membrane skeleton: recent progress. *Blood.* 61:1–11.
17. Lin, D. C., and S. Lin. 1979. Actin polymerization induced by a motility related high affinity binding complex from human erythrocyte membranes. *Proc. Natl. Acad. Sci. USA.* 76:2345–2349.
18. Ungewickell, E., P. M. Bennett, R. Calvert, V. Ohanian, and W. B. Gratzer. 1979. In vitro formation of a complex between cytoskeletal proteins of the human erythrocyte. *Nature (Lond.).* 280:811–814.
19. Brenner, S. L., and E. D. Korn. 1980. Spectrin-actin complex isolated from sheep erythrocytes accelerates actin polymerization by simple nucleation: evidence for oligomeric actin in the erythrocyte cytoskeleton. *J. Biol. Chem.* 255:1670–1676.
20. Atkinson, M. A. L., J. S. Morrow, and V. T. Marchesi. 1982. The polymeric state of actin in the human erythrocyte cytoskeleton. *J. Cell. Biochem.* 18:493–505.
21. Pinder, J. C., and W. B. Gratzer. 1983. Structure and dynamic states of actin in the erythrocyte. *J. Cell Biol.* 96:768–775.
22. Brenner, S. L., and E. D. Korn. 1979. Spectrin-actin interaction: phosphorylated and dephosphorylated spectrin tetramers cross-link F-actin. *J. Biol. Chem.* 254:8620–8627.
23. Cohen, C. M., J. M. Tyler, and D. Branton. 1980. Spectrin-actin associations studied by electron microscopy of shadowed preparations. *Cell.* 21:875–883.
24. Fowler, V., and D. L. Taylor. 1980. Spectrin plus band 4.1 cross-link actin: regulation by micromolar calcium. *J. Cell Biol.* 85:361–376.
25. Cohen, C., and S. Foley. 1982. The role of band 4.1 in the association of actin with erythrocyte membranes. *Biochim. Biophys. Acta.* 688:691–701.
26. Tyler, J. M., B. N. Reinhardt, and D. Branton. 1980. Associations of erythrocyte membrane proteins: binding of purified bands 2.1 and 4.1 to spectrin. *J. Biol. Chem.* 255:7034–7039.
27. Mueller, T. J., and M. Morrison. 1981. Glycoconnectin (PAS-2), a membrane attachment site for the human erythrocyte cytoskeleton. *In* Erythrocyte Membranes 2: Recent Clinical and Experimental Advances. W. Kruchberg, J. Easton, and G. Brewer, editors. Alan R. Liss, New York. 95–112.
28. Lux, S. E. 1979. Dissecting the erythrocyte membrane cytoskeleton. *Nature (Lond.).* 281:426–429.
29. Gratzer, W. B. 1981. The red cell membrane and its cytoskeleton. *Biochem. J.* 198:1–8.
30. Bennett, V. 1982. The molecular basis for membrane-cytoskeleton association in human erythrocytes. *J. Cell Biochem.* 18:49–65.
31. Goodman, S. R., and K. Shiffer. 1983. The spectrin membrane skeleton of normal and abnormal human erythrocytes: a review. *Am. J. Physiol.* 244:C121–C141.
32. Cohen, C. 1983. The molecular organization of the red cell membrane skeleton. *Semin. Hematol.* 20:141–158.
33. Gratzer, W. B. 1983. The Cytoskeleton of the Red Blood Cell. *In* Muscle and Nonmuscle Motility. A. Stracher, editor. Academic Press, Inc., New York. 2:37–125.
34. Shen, B. W., R. Josephs, and T. L. Steck. 1983. Visualization of actin protofilaments in the skeleton of the human erythrocyte membrane. *Fed. Proc.* 42:2196*a*. (Abstr.)
35. Martin, T. E., and I. G. Wool. 1969. Active hybrid 80 S particles formed from subunits of rat, rabbit and protozoan (Tetrahymena pyrifomis) ribosomes. *J. Mol. Biol.* 43:151–161.
36. Spudich, J. A., and S. Watt. 1971. The regulation of rabbit skeletal muscle contraction. *J. Biol. Chem.* 246:4866–4871.
37. Weeds, A. G., and R. S. Taylor. 1975. Separation of subfragment-1 isoenzymes from rabbit skeletal muscle myosin. *Nature (Lond.).* 257:54–56.
38. Fairbanks, G., T. L. Steck, and D. F. H. Wallach. 1971. Electrophoretic analysis of the major polypeptides of the human erythrocyte membrane. *Biochemistry.* 10:2606–2617.
39. Steck, T. L., and J. Yu. 1973. Selective solubilization of proteins from red blood cell membranes by protein perturbants. *J. Supramol. Struct.* 1:220–232.
40. Moore, P. B., H. E. Huxley, and D. J. DeRosier. 1970. Three-dimensional reconstruction of F-actin, thin filaments and decorated thin filaments. *J. Mol. Biol.* 50:279–295.
41. Meek, G. A. 1978. Practical Electron Microscopy for Biologists. John Wiley and Sons, New York. Second ed. 298–324.
42. Ralston, G. B., J. Dunbar, and M. White. 1977. The temperature-dependent dissociation of spectrin. *Biochim. Biophys. Acta.* 491:345–348.
43. Ungewickell, E., and W. Gratzer. 1978. Self-association of human spectrin: a thermodynamic and kinetic study. *Eur. J. Biochem.* 88:379–385.
44. Ungewickell, E., and D. Branton. 1982. Triskelions: the building blocks of clathrin coats. *Trends Biochem. Sci.* 7:358–361.
45. Liu, S. C., P. Windisch, S. Kim, and J. Palek, 1983. Oligomeric species of spectrin in extracts of normal erythrocyte membranes. *J. Cell Biol.* 97(5, Pt. 1):284*a*. (Abstr.)
46. Kirchhausen, T., and S. C. Harrison. 1981. Protein organization in clathrin trimers. *Cell* 23:755–761.
47. Kondo, H., and S. Ishiwata. 1976. Unidirectional growth of F-actin. *J. Biochem.* 79:159–171.
48. Woodrum, D. T., S. A. Rich, and T. D. Pollard. 1975. Evidence for biased bidirectional polymerization of actin filaments using heavy meromyosin prepared by an improved method. *J. Cell Biol.* 67:231–237.
49. Morrow, J. S., and V. T. Marchesi. 1981. Self-assembly of spectrin oligomers in vitro: a basis for a dynamic cytoskeleton. *J. Cell Biol.* 88:463–468.
50. Siegel, D. L., and D. Branton. 1983. Human erythrocyte band 4.9, an actin bundling protein. *J. Cell Biol.* 97(5, Pt. 2):279*a*. (Abstr.)
51. Egelman, E. H., N. Francis, and D. J. De Rosier. 1982. F-actin is a helix with a random variable twist. *Nature (Lond.).* 298:131–135.
52. Estes, J. E., L. A. Seldon, and L. C. Gershman. 1981. Mechanism of action of phalloidin on the polymerization of muscle actin. *Biochemistry.* 20:708–712.
53. Cohen, C. M., and D. Branton. 1979. The role of spectrin in erythrocyte membrane-stimulated actin polymerisation. *Nature (Lond.).* 279:163–165.
54. Bonder, E. M., D. J. Fishkind, and M. S. Mooseker. 1983. Direct measurement of critical concentrations and assembly rate constants at the two ends of an actin filament. *Cell.* 34:491–501.
55. Wegner, A., and G. Isenberg. 1983. 12-fold difference between the critical monomer concentrations of the two ends of actin filaments in physiological salt conditions. *Proc. Natl. Acad. Sci. USA.* 80:4922–4925.
56. Tsukita, S., S. Tsukita, and H. Ishikawa. 1984. Bidirectional polymerization of G-actin on the human erythrocyte membrane. *J. Cell Biol.* 98:1102–1110.
57. Becker, P. S., J. E. Spiegel, L. C. Wolfe, and S. E. Lux. 1983. High yield purification of protein 4.1 from human erythrocyte membranes. *Anal. Biochem.* 132:195–201.
58. Lin, D. C. 1981. Spectrin-4.1-actin complex of the human erythrocyte: molecular basis of its ability to bind cytochalasins with high-affinity and to accelerate actin polymerization in vitro. *J. Supramol. Struct. Cell. Biochem.* 15:129–138.
59. Fowler, V. M., and V. B. Bennett. 1983. Erythrocyte membrane tropomyosin. *J. Cell Biol.* 97(5, Pt. 2):208*a*. (Abstr.)
60. Huxley, H. E., and W. Brown. 1967. The low angle x-ray diagram of vertebrate striated muscle and its behavior during contraction and rigor. *J. Mol. Biol.* 30:383–434.
61. Cote, G. P., and L. B. Smillie. 1981. Preparation and some properties of equine platelet tropomyosin. *J. Biol. Chem.* 256:11004–11010.
62. Fowler, V. M., and V. B. Bennett. 1984. *In* Workshop on Erythrocyte Membranes. G. J. Brewer, editor. Alan R. Liss, Inc., New York. In press.
63. Cohen, C. M., and S. F. Foley. 1983. Stoichiometry of complex formation between human erythrocyte spectrin, band 4.1 and actin. *J. Cell Biol.* 97(5, Pt. 2):283*a*. (Abstr.)